AN EFFECTIVE SOLUTION OF THE COMPOSITE (FGM'S) BEAM STRUCTURES

Justín Murín, Vladimír Kutiš*

The additive mixture rules have been extended for calculation of the effective longitudinal elasticity modulus of the composite (Functionally Graded Materials – FGM's) beams with both the polynomial longitudinal variation of the constituent's volume fraction and polynomial longitudinal variation of the constituent's elasticity modulus. Stiffness matrix of the composite Bernoulli-Euler beam has been established which contains the transfer constants. These transfer constants describe very accurately the polynomial uni-axially variation of the effective longitudinal elasticity modulus, which is calculated using the extended mixture rules.

The mixture rules have been extended for calculation of the effective elasticity modulus for stretching and flexural bending of the layer-wise symmetric composite (FGM's) sandwich beam finite element as well. The polynomial longitudinal and transversally symmetric layer-wise variation of the sandwich beam stiffness has been taken into the account. Elastic behaviour of the sandwich beam will be modelled by the laminate theory. Stiffness matrix of such new sandwich beam element has been established. The nature and quality of the matrix-reinforcement interface have not been considered. Four examples have been solved using the extended mixture rules and the new composite (FGM's) beam elements with varying stiffness. The obtained results are evaluated, discussed and compared.

Key words: *composite beam finite element, sandwich beam, functionally graded materials, mixture rules*

1. Motivation

Composite structure elements, like the laminate, sandwich, or FGM's beams with the simple or double symmetric cross-sections are very important in engineering applications. Macro-mechanical modelling and analysis of the composites are based on the homogenisation of material properties. Micro-mechanical modelling leads to a correlation between properties of the constituents and the average effective properties of composite. Mixture rules are used in the engineering applications for the derivation of average material properties. These rules of mixture are based on the statement that the composite longitudinal property (Young's modulus, Poisson's ratio, coefficient of thermal and electrical conduction) is the sum of the properties of each constituent multiplied by its volume fraction. To increase the accuracy of the composite material properties calculation, new homogenisation techniques and improved mixture rules have been applied (for example [1, 2, 3]).The multiscale computation represents the most actual trend in the homogenisation [4, 5].

In many publications, for example [6], the constant volume fractions and material properties of the composite constituents in the whole composite beam have been considered. The

* prof. Ing. J. Murín, DrSc., Ing. V. Kutiš, Ph.D., Slovak University of Technology, Faculty of Electrical Engineering and Information Technology, Department of Mechanics, Bratislava, 812 19 Slovak Republic

similar consideration is made for sandwich beams, where the constant properties in each layer were assumed. But in several current papers, for example in [7], new beam finite elements for static and dynamic analyses of beam structures with varying thermal and elastic properties along the beam thickness has been presented. To the best of author's knowledge, no finite element formulation is available in the literature for FGM beam with either longitudinal or with the both longitudinal and transversal variation of material properties.

The main topic of this contribution lies in extension of the mixture rules for deriving of the effective longitudinal elasticity modulus of composite beam with varying stiffness. Firstly, a longitudinal polynomial variation of volume fractions and elasticity modulus of the composite constituents will be considered. Secondly, both longitudinal and symmetric transversal layer-wise variation of the above-mentioned material parameters will be assumed. The elastic behaviour of this sandwich beam will be modelled by the laminate theory. The nature and quality of the matrix-reinforcement interface have not been taken into the account. Four numerical examples have been solved using the extended mixture rules and the new FGM beam elements with varying stiffness. The analysis results will be evaluated, discussed and compared with those obtained using the beam and solid finite elements of the FEM-program ANSYS [8], where a very fine mesh of these elements with varying material properties had to be used.

2. Derivation of an effective longitudinal elasticity modulus

The 2D Bernoulli-Euler beam finite element of composite or FGM's is depicted in Figure 1. The material of the composite beam consists of the matrix and the fibres. The FGM of such a beam element consists of two or more constituents that have been built together by powder metallurgy, for example. Variation of the material properties can be caused by the varying percentage (volume fraction) of constituents and/or by variation of their material properties (which is caused by varying temperature field, for example). Then, the new materials will have graded properties in spatial direction. Longitudinal variation of the volume fractions and longitudinal variation of the elasticity modulus of constituents will be assumed in this chapter. The material properties will be assumed constant along the beam width and depth. A constant cross-sectional area can have various geometries but it has to be symmetric to the bending (x-y) plane. The symmetric transversal layer-wise stiffness variation of the sandwich beam element will be assumed in the part 3 of this paper. Longitudinal variation of the stiffness of layers will be considered by this sandwich beam element, as well.

2.1. Composite beam with uni-axially varying volume fractions

We assume constant values of the elasticity moduli of the fibres and the matrix (or the two FGM constituents) in the beam element: $E_{\mathrm{f}} = \text{const.}$; $E_{\mathrm{m}} = \text{const.}$. The fibre volume fraction $v_{\mathrm{f}}(x)$ is chosen as a polynomial function of x:

$$v_{\mathrm{f}}(x) = 1 - v_{\mathrm{m}}(x) = v_{\mathrm{f}i}\,\eta_{\mathrm{vf}}(x) = v_{\mathrm{f}i}\left(1 + \sum_{k=1}^{r} \eta_{\mathrm{vf}k}\,x^k\right) . \tag{1}$$

The matrix volume fraction $v_{\mathrm{m}}(x)$ is then

$$v_{\mathrm{m}}(x) = 1 - v_{\mathrm{f}}(x) = v_{\mathrm{m}i}\,\eta_{\mathrm{vm}}(x) = v_{\mathrm{m}i}\left(1 + \sum_{k=1}^{r} \eta_{\mathrm{vm}k}\,x^k\right) \tag{2}$$

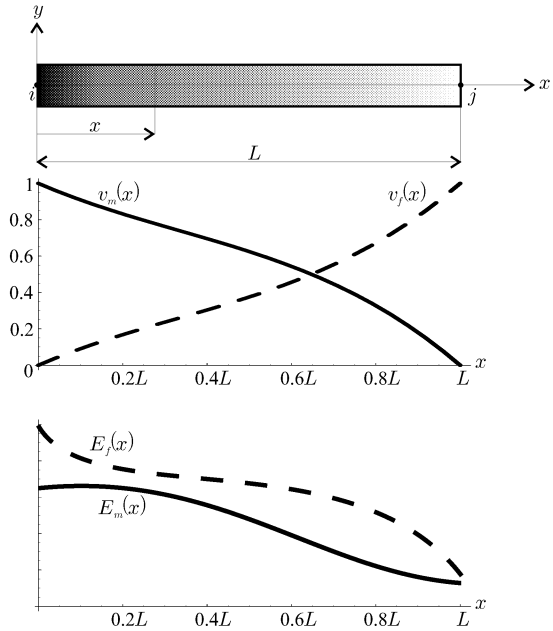

Fig.1: Composite beam element with longitudinal variation of volume fractions and elasticity moduli of the constituents

where $v_{\mathrm{f}i}$ and $v_{\mathrm{m}i}$ are the fibre and the matrix volume fractions at node i, respectively. $\eta_{\mathrm{vf}}(x)$ and $\eta_{\mathrm{vm}}(x)$ are the polynomial of fibre and matrix volume fractions variation, respectively. The constants $\eta_{\mathrm{vf}k}$ and $\eta_{\mathrm{vm}k}$, $(k = 1, \ldots, r)$, and the order r of these polynomials depend on the variation of the fibre and the matrix volume fractions. The effective longitudinal elasticity modulus $E_{\mathrm{L}}(x)$ can be derived using the extended additive mixture rule as

$$E_{\mathrm{L}}(x) = v_{\mathrm{f}}(x)\, E_{\mathrm{f}} + v_{\mathrm{m}}(x)\, E_{\mathrm{m}} \ . \tag{3}$$

After some manipulation we get

$$E_{\mathrm{L}}(x) = E_{\mathrm{L}i}\, \eta_{E_{\mathrm{L}}}(x) \tag{4}$$

where $E_{\mathrm{L}i} = v_{\mathrm{f}i}\, E_{\mathrm{f}} + (1 - v_{\mathrm{f}i})\, E_{\mathrm{m}}$ is the effective elasticity modulus at node i, and

$$\eta_{E_{\mathrm{L}}}(x) = 1 + \frac{E_{\mathrm{f}}\, v_{\mathrm{f}i} \sum\limits_{k=1}^{r} \eta_{\mathrm{vf}k}\, x^k + E_{\mathrm{m}}\, v_{\mathrm{m}i} \sum\limits_{k=1}^{r} \eta_{\mathrm{vm}k}\, x^k}{E_{\mathrm{L}i}} \tag{5}$$

is the polynomial of the effective longitudinal elasticity modulus variation.

Example 1:

Now we consider a cantilever composite beam loaded by axial and lateral forces $F = 1\,\mathrm{N}$ (Figure 2). The material of this beam is a mixture of the matrix (epoxy – with the elasticity modulus $E_{\mathrm{m}} = \text{const.} = 3\,\mathrm{GPa}$) and fibres (E-glass – with the elasticity modulus $E_{\mathrm{f}} = \text{const.} = 72.4\,\mathrm{GPa}$). The varying fibre volume fraction (1) is chosen as a quadratic polynomial

$$v_{\mathrm{f}}(x) = 0.5\,(1 + 0.9\,x - 0.4\,x^2) \ .$$

The varying matrix volume fraction (2) was then obtained as (Figure 3A)

$$v_{\mathrm{m}}(x) = 0.5\,(1 - 0.9\,x + 0.4\,x^2)\ .$$

From (3) we get the polynomial variation of the effective longitudinal elasticity modulus (4)

$$E_{\mathrm{L}}(x) = 37.7\,(1 + 0.8284\,x - 0.3682\,x^2)\ [\mathrm{GPa}]\ ,$$

where $E_{\mathrm{L}i} = 37.7\,\mathrm{GPa}$ and $E_{\mathrm{L}j} = 55.05\,\mathrm{GPa}$ (Figure 3B).

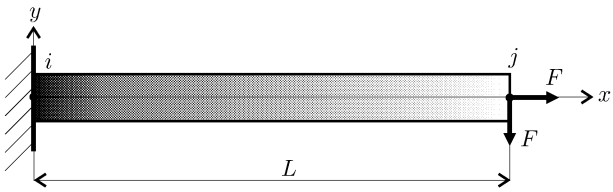

Fig.2: Cantilever composite beam

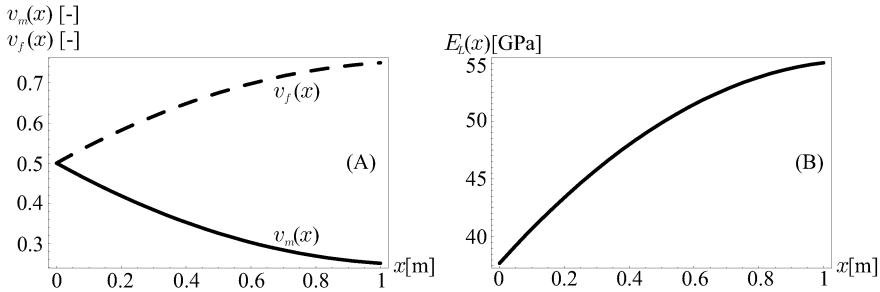

Fig.3: Components volume fractions (A), effective elasticity modulus (B)

The cross-section is a square ($0.05\times0.05\,\mathrm{m}$) with an area of $A = 0.0025\,\mathrm{m}^2$, $I = 5.2083\times10^{-7}\,\mathrm{m}^4$ is the quadratic area moment of inertia. The length of the beam is $L = 1\,\mathrm{m}$.

The axial and transversal displacements have been obtained from the local linear elastic (Bernoulli-Euler) beam finite element stiffness relation [9] that has now the following form for the FGM beam

$$\begin{bmatrix} \frac{E_{\mathrm{L}i}\,A}{d'_{2\mathrm{AE}}} & 0 & 0 & -\frac{E_{\mathrm{L}i}\,A}{d'_{2\mathrm{AE}}} & 0 & 0 \\ 0 & c\,b'_{2\mathrm{EI}} & c\,b'_{3\mathrm{EI}} & 0 & -c\,b'_{2\mathrm{EI}} & c\,b_{2\mathrm{EI}} \\ 0 & c\,b'_{3\mathrm{EI}} & c\,(L\,b'_{3\mathrm{EI}} - b_{3\mathrm{EI}}) & 0 & -c\,b'_{3\mathrm{EI}} & c\,b_{3\mathrm{EI}} \\ -\frac{E_{\mathrm{L}i}\,A}{d'_{2\mathrm{AE}}} & 0 & 0 & \frac{E_{\mathrm{L}i}\,A}{d'_{2\mathrm{AE}}} & 0 & 0 \\ 0 & -c\,b'_{2\mathrm{EI}} & -c\,b'_{3\mathrm{EI}} & 0 & c\,b'_{2\mathrm{EI}} & -c\,b_{2\mathrm{EI}} \\ 0 & c\,b_{2\mathrm{EI}} & c\,b_{3\mathrm{EI}} & 0 & -c\,b_{2\mathrm{EI}} & c\,(L\,b_{2\mathrm{EI}} - b_{3\mathrm{EI}}) \end{bmatrix} \begin{bmatrix} u_i \\ v_i \\ \varphi_i \\ u_j \\ v_j \\ \varphi_j \end{bmatrix} = \begin{bmatrix} R_{\mathrm{x}} \\ R_{\mathrm{y}} \\ M_{\mathrm{z}} \\ F \\ -F \\ 0 \end{bmatrix}$$

where $c = E_{\mathrm{L}i}\,I/(b_{2\mathrm{EI}}\,b'_{3\mathrm{EI}} - b_{3\mathrm{EI}}\,b'_{2\mathrm{EI}})$ is the bending stiffness constant. The transfer constants $b'_{2\mathrm{EI}}$, $b'_{3\mathrm{EI}}$, $b_{2\mathrm{EI}}$ and $b_{3\mathrm{EI}}$, which can be calculated using a simple numerical algorithm [10, 11], depend on the cross-sectional characteristics and effective longitudinal elasticity modulus variation.

A vector of unknown parameters contains displacements in x direction u_i, u_j, displacements in y direction v_i, v_j and rotations around z axis φ_i and φ_j. The right-hand side of this relation represents axial and transversal forces, and in-plane moments (external loads at node j and reactions at node i). Figure 4 shows axial displacements and strains of the

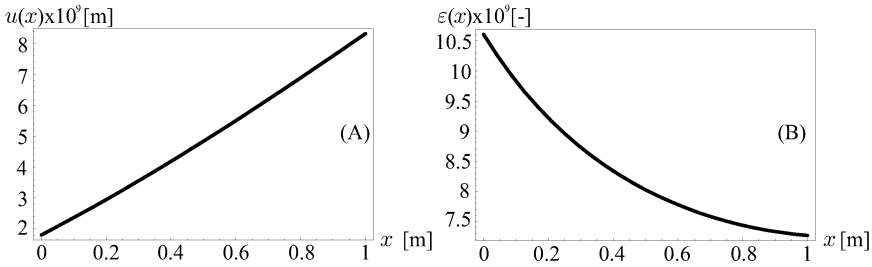

Fig.4: Axial displacements (A) and strains (B)

beam caused by the axial force F. As it can be seen (Figure 4), their dependence on x is non-linear. The maximal axial displacement is $u_j = 0.83135{\times}10^{-8}$ m and the maximal axial strain is $\varepsilon_i = 1.0610{\times}10^{-8}$. The average axial stress is equal to 400 Pa and it will be constant along the beam length. Figure 5 shows the deflection of this beam caused by the lateral force F. The deflection and the rotation at the free beam end are $v_j = -1.4668{\times}10^{-5}$ m and $\varphi_j = -2.1199{\times}10^{-5}$ rad respectively. The reactions at node i satisfy fully the equilibrium equations. The same task has been solved with the finite element BEAM3 (ANSYS [8]),

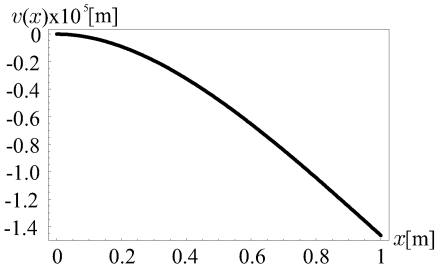

Fig.5: Deflection curve of the cantilever beam with varying volume fractions

where the number of elements has been increased. When the whole beam was divided into 200 elements, the analysis results were in good agreement with the results obtained with only one new finite element. The average Young's modulus of each BEAM3 element has been stated from the effective elasticity modulus $E_{\mathrm{L}}(x)$. The ANSYS analysis results are: maximal value of the axial displacement (caused by axial force) at the free end of the beam has the value of $u_j = 0.83135{\times}10^{-8}$ m; the maximal value of axial strain at the clamped end of this beam is $\varepsilon_i = 1.0588{\times}10^{-8}$; the maximal deflection (Figure 5) and rotation (caused by the vertical force) at the free beam end are $v_j = -1.4641{\times}10^{-4}$ m and $\varphi_j = -2.1196{\times}10^{-5}$ rad respectively. It can be seen that the axial displacements, the strains and the deflection curve are in a very good agreement with those depicted in Figure 4 and 5, if a very fine mesh of the BEAM3 element has been used.

2.2. Composite beam with uni-axially varying elasticity moduli of the constituents

Let us consider constant values of the fibre and the matrix volume fractions: $v_\mathrm{f} = \mathrm{const.}$; $v_\mathrm{m} = \mathrm{const.}$. The fibre elasticity modulus $E_\mathrm{f}(x)$ and the matrix elasticity modulus $E_\mathrm{m}(x)$ are chosen as polynomial functions of x:

$$E_\mathrm{f}(x) = E_{\mathrm{f}i}\,\eta_\mathrm{Ef}(x) = E_{\mathrm{f}i}\left(1 + \sum_{k=1}^{r} \eta_{\mathrm{Ef}k}\,x^k\right)\,, \tag{6}$$

$$E_\mathrm{m}(x) = E_{\mathrm{m}i}\eta_\mathrm{Em}(x) = E_{\mathrm{m}i}\left(1 + \sum_{k=1}^{s} \eta_{\mathrm{Em}k}\,x^k\right)\,. \tag{7}$$

$E_{\mathrm{f}i}$ and $E_{\mathrm{m}i}$ are the fibre and the matrix elasticity moduli at node i, respectively. $\eta_\mathrm{Ef}(x)$ is the polynomial of fibre elasticity modulus variation. Its constants $\eta_{\mathrm{Ef}k}$, where $k = 1, \ldots, r$, and order r of this polynomial depend on the fibre elasticity modulus variation. $\eta_\mathrm{Em}(x)$ is the polynomial of matrix elasticity modulus variation. The constants $\eta_{\mathrm{Em}k}$, where $k = 1, \ldots, s$, and the order s of this polynomial depend on the matrix elasticity modulus variation. The effective longitudinal elasticity modulus is

$$E_\mathrm{L}(x) = v_\mathrm{f}\,E_\mathrm{f}(x) + v_\mathrm{m}\,E_\mathrm{m}(x)\,. \tag{8}$$

Similarly to (4), we can write

$$E_\mathrm{L}(x) = E_{\mathrm{L}i}\,\eta_{E_\mathrm{L}}(x) \tag{9}$$

where $E_{\mathrm{L}i} = v_\mathrm{f}\,E_{\mathrm{f}i} + (1 - v_\mathrm{f})\,E_{\mathrm{m}i}$ is the effective elasticity modulus at node i, and

$$\eta_{E_\mathrm{L}}(x) = 1 + \frac{E_{\mathrm{f}i}\,v_\mathrm{f}\sum\limits_{k=1}^{r}\eta_{\mathrm{Ef}k}\,x^k + E_{\mathrm{m}i}\,v_\mathrm{m}\sum\limits_{k=1}^{s}\eta_{\mathrm{Em}k}\,x^k}{E_{\mathrm{L}i}} \tag{10}$$

is the polynomial of effective longitudinal elasticity modulus variation.

Example 2:

Now let us consider a cantilever composite beam with the same geometry, loads and constrains as above (Figure 2). The volume of this beam is filled with a mixture of matrix (epoxy – with the volume fraction $v_\mathrm{m} = \mathrm{const.} = 0.7$) and fibres (E-glass – with the volume fraction $v_\mathrm{f} = \mathrm{const.} = 0.3$). The varying fibre elasticity modulus (6) is chosen as

$$E_\mathrm{f}(x) = 72.4\,(1 - 0.5\,x + 0.01\,x^2)\ [\mathrm{GPa}]\,.$$

The varying matrix elasticity modulus (7) is chosen as

$$E_\mathrm{m}(x) = 3.0\,(1 - 0.5\,x + 0.01\,x^2)\ [\mathrm{GPa}]\,.$$

From (8) we get the polynomial variation of an effective longitudinal elasticity modulus (9)

$$E_\mathrm{L}(x) = 51.58\,(1 - 0.5\,x + 0.01\,x^2)\ [\mathrm{GPa}]$$

where $E_{\mathrm{L}i} = 51.58\,\mathrm{GPa}$ and $E_{\mathrm{L}j} = 26.3058\,\mathrm{GPa}$. All the three variations of the elasticity moduli are shown in Figure 6.

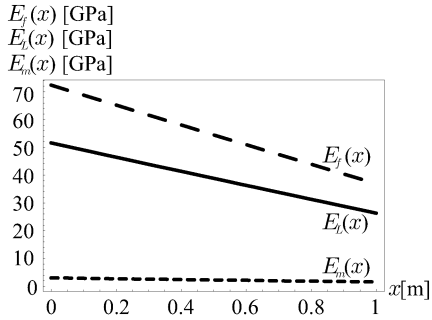

Fig.6: Elasticity modulus variations

The axial and transversal displacements have been obtained from the same local linear elastic beam finite element stiffness relation as above. Figure 7 shows the axial displacements and the axial strains of the beam caused by the axial force. The maximal axial displacement is $u_j = 1.06809\times10^{-8}$ m, the maximal axial strain is $\varepsilon_j = 1.5205\times10^{-8}$. The average axial stress equals to 400 Pa and it will be constant along the x-axis.

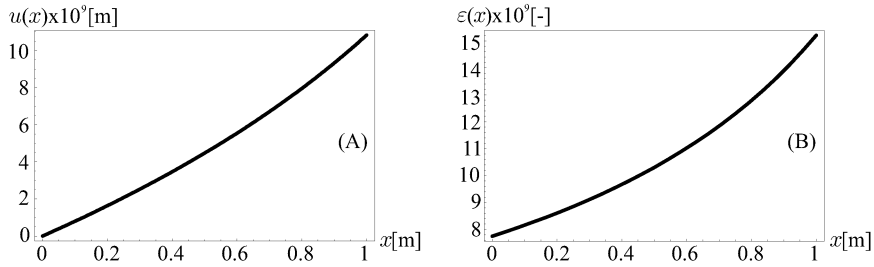

Fig.7: Axial displacements (A) and strain (B) of the beam with varying moduli of components

Figure 8 shows the deflection of this beam caused by the lateral force. The deflection and rotation at the free end of this beam are $v_j = -1.4356\times10^{-5}$ m and $\varphi_j = -2.2777\times10^{-5}$ rad, respectively. The reactions at node i exactly fulfiled the equilibrium equations.

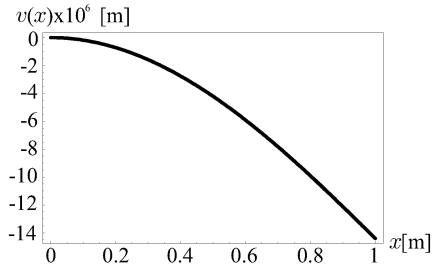

Fig.8: Deflection curve of the beam with varying elasticity moduli of components

The same task has been solved with the BEAM3 finite element using the same mesh density as in the Example 1. The following results have been obtained: maximal value of the axial displacement is $u_j = 1.0822\times10^{-8}$ m and the adequate strain is

$\varepsilon_j = 1.5785\times10^{-8}$; maximal value of the deflection and rotation is $v_j = -1.4403\times10^{-5}\,\mathrm{m}$ and $\varphi_j = -2.2912\times10^{-5}\,\mathrm{rad}$, respectively. The obtained axial displacements and deflection curve agree well with those obtained using only one new beam finite element.

2.3. Composite beam with the uni-axially varying elasticity moduli and volume fractions of the constituents

We assume polynomial variation of the fibre and matrix volume fractions that are given by expressions (1) and (2). The fibre elasticity modulus $E_f(x)$ and the matrix elasticity modulus $E_m(x)$ are chosen as polynomial functions of x too; see expressions (6) and (7).

Then the effective longitudinal elasticity modulus of the composite beam is given by

$$E_{\mathrm{L}}(x) = v_{\mathrm{f}}(x)\,E_{\mathrm{f}}(x) + v_{\mathrm{m}}(x)\,E_{\mathrm{m}}(x)\ . \tag{11}$$

Similarly to (4), we can write

$$E_{\mathrm{L}}(x) = E_{\mathrm{L}i}\,\eta_{E_{\mathrm{L}}}(x) \tag{12}$$

where $E_{\mathrm{L}i} = v_{\mathrm{f}i}\,E_{\mathrm{f}i} + (1 - v_{\mathrm{f}i})\,E_{\mathrm{m}i}$ is the effective longitudinal elasticity modulus at node i, and

$$\eta_{E_{\mathrm{L}}}(x) = 1 + \frac{\eta_{\mathrm{vf}}(x)\,\eta_{\mathrm{Ef}}(x) + \eta_{\mathrm{vm}}(x)\,\eta_{\mathrm{Em}}(x)}{E_{\mathrm{L}i}} \tag{13}$$

is the polynomial of effective longitudinal elasticity modulus variation.

Example 3:

For the beam (Figure 2) the varying fibre volume fraction (1) is chosen as

$$v_f(x) = 0.5\,(1 - 0.5\,x + 0.001\,x^2)\ .$$

The varying matrix volume fraction (2) we get is

$$v_{\mathrm{m}}(x) = 0.5\,(1 + 0.5\,x - 0.001\,x^2)\ .$$

The varying fibre elasticity modulus (6) is chosen as

$$E_{\mathrm{f}}(x) = 72.4\,(1 - 0.5\,x + 0.01\,x^2)\ [\mathrm{GPa}]\ .$$

The varying matrix elasticity modulus (7) is chosen as

$$E_{\mathrm{m}}(x) = 3.0\,(1 - 0.5\,x + 0.01\,x^2)\ [\mathrm{GPa}]\ .$$

From (10) we get the polynomial variation of the effective longitudinal elasticity modulus (11)

$$E_{\mathrm{L}}(x) = E_{\mathrm{L}i}\,(1 - 0.960\,x + 0.241\,x^2 - 0.005\,x^3 + 0.920\times10^{-5}\,x^4)$$

where $E_{\mathrm{L}i} = 37.7\,\mathrm{GPa}$ and $E_{Lj} = 10.396\,\mathrm{GPa}$.

Figure 9 shows distributions of volume fractions, elasticity moduli of the constituents and the longitudinal effective modulus of the composite beam. The axial and transversal displacements have been obtained from the same local linear elastic beam finite element stiffness relation as above.

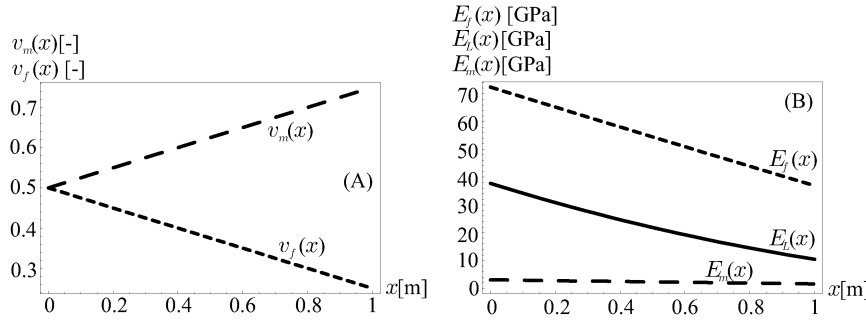

Fig.9: Volume fractions (A) and elasticity moduli (B) of constituents

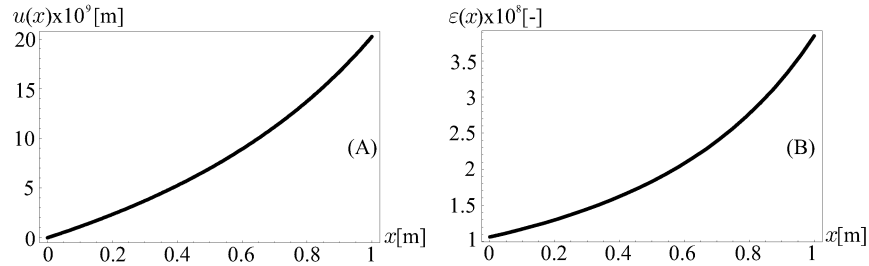

Fig.10: Axial displacements (A) and strains (B) of the beam with varying volume fractions and elasticity moduli

Figure 10 shows the axial displacements and strains of the beam caused by the axial force.

The maximal axial displacement is $u_j = 2.0251{\times}10^{-8}$ m, the maximal axial strain is $\varepsilon_j = 3.8475{\times}10^{-8}$. The average axial stress is constant and equals to 400 Pa.

Figure 11 shows the deflection curve of this beam caused by the lateral force. The deflection and rotation at the free beam end is $v_j = -2.2758{\times}10^{-5}$ m and $\varphi_j = -3.8306{\times}10^{-5}$ rad respectively. It can be shown that the reactions at node i fulfil the equilibrium equations exactly.

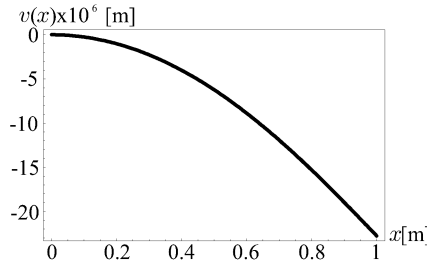

Fig.11: Deflection curve of the beam with varying volume fractions and elasticity moduli

To compare the accuracy and effectiveness of our new composite beam element, the 200 BEAM3 elements with varying elasticity modulus $E_{\mathrm{L}}(x)$ have been used for solving the above example.

Using this fine mesh of the BEAM3 beam elements a very good agreement of results of the both analyses has been obtained. The maximal values of axial displacement and strain at the free end of this beam are $u_j = 2.0244\times10^{-5}\,\mathrm{m}$ and $\varepsilon_j = 3.8270\times10^{-8}$, respectively. The following maximal values of deflection and rotation have been obtained: $v_j = 2.2758\times10^{-5}\,\mathrm{m}$, $\varphi_j = 3.8307\times10^{-5}\,\mathrm{rad}$.

3. Longitudinal elasticity modulus for the symmetric sandwich beam element with the longitudinal and symmetric transversal layer-wise varying stiffness

Let us consider a sandwich straight beam with double symmetric cross-sections A that are predominantly rectangular. The beam is loaded orthogonally to the plane of lamination. Debonding of layers is not considered. If the lamination is symmetric, the elementary theory of homogeneous isotropic beams can be used for all solutions, but the elasticity modulus has to be replaced by its effective value [6]. The single layers are built from composite material with longitudinal variation of the volume fractions and elasticity modulus of the constituents as described in part 2. The two-node beam element (Figure 12) with three composite layers has the following geometric and material properties:

- $A_1 = A_3$, A_2 are cross-sections of the layers, where $v_1 = v_3 = A_1/A$, $v_2 = A_2/A$ are volume fractions of layers in the sandwich beam,
- $E_1(x) = E_{1i}\,\eta_{\mathrm{E}1}(x) = E_{1i}\left(1+\sum_{k=1}^{r}\eta_{\mathrm{E}1k}\,x^k\right) = E_3(x) = E_{3i}\,\eta_{\mathrm{E}3}(x) = E^{\mathrm{f}}(x)$ is an effective longitudinal elasticity modulus of layers 1 and 3 (faces),
- $E_2(x) = E_{2i}\,\eta_{\mathrm{E}2}(x) = E_{2i}\left(1+\sum_{l=1}^{s}\eta_{\mathrm{E}2l}\,x^l\right) = E^{\mathrm{c}}(x)$ is an effective longitudinal elasticity modulus of layer 2 (core),
- $\mathrm{E}_{1i} = E_{3i}$, E_{2i} are effective longitudinal elasticity moduli of layers 1, 3, and 2 at node i, respectively,
- $\eta_{\mathrm{E}1}(x) = \eta_{\mathrm{E}3}(x)$ and $\eta_{\mathrm{E}2}(x)$ are the polynomial variations of the effective longitudinal elasticity moduli of layers 1, 3 and 2, respectively,
- Layers 1 and 3 (faces) have the same thicknesses h^{f} and they are of the same material; layer 2 (core) has thickness h^{c}. Parameter $d = h^{\mathrm{c}} + h^{\mathrm{f}}$.

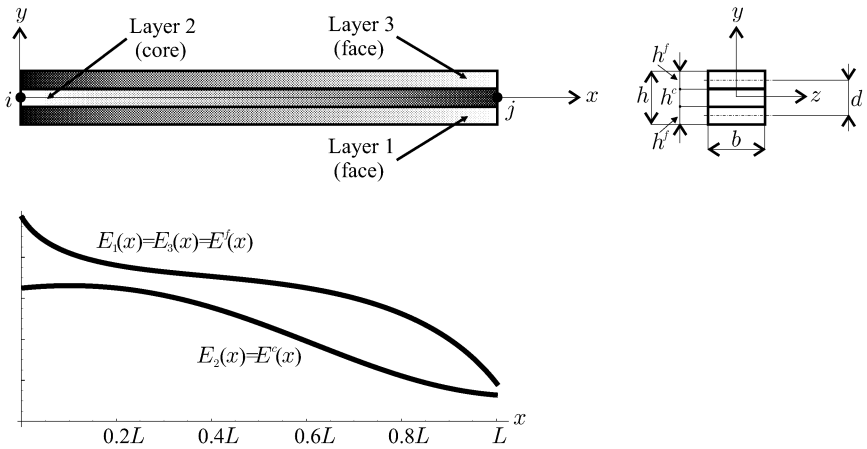

Fig.12: Symmetric sandwich (three layers) composite beam

Using the mixture rule, the effective longitudinal elasticity modulus for stretching is

$$E_{\mathrm{L}}^{\mathrm{N}}(x) = \sum_{n=1}^{3} v_{\mathrm{n}}\, E_{\mathrm{n}}(x) = E_{\mathrm{LN}i}\, \eta_{\mathrm{ELN}}(x) \tag{14}$$

where $E_{\mathrm{LN}i} = E_{1i}\, v_1 + E_{2i}\, v_2 + E_{3i}\, v_3$ is an effective longitudinal elasticity modulus for stretching at node i, $\eta_{\mathrm{ELN}}(x)$ is the polynomial variation of the effective longitudinal elasticity modulus for stretching of the sandwich beam. The advanced effective longitudinal elasticity modulus for flexural loading of the sandwich beam, according the laminate theory [6], is

$$E_{\mathrm{L}}^{\mathrm{M}}(x) = \frac{12}{h^3}\left(\frac{E^{\mathrm{f}}(x)\,(h^{\mathrm{f}})^3}{6} + \frac{E^{\mathrm{f}}(x)\,h^{\mathrm{f}}\,(h^{\mathrm{c}}+h^{\mathrm{f}})^2}{2} + \frac{E^{\mathrm{c}}(x)\,(h^{\mathrm{c}})^3}{12}\right) = E_{\mathrm{LM}i}\,\eta_{\mathrm{ELM}}(x)\ . \tag{15}$$

Here, $E_{\mathrm{LM}i}$ is an effective elasticity modulus for flexural loading at node i, $\eta_{\mathrm{ELM}}(x)$ is its polynomial variation, $h = h^{\mathrm{c}} + 2\,h^{\mathrm{f}}$ is the total beam depth. Elasticity moduli (14) and (15) affect the stiffness matrix parameters of the new sandwich beam element with varying stiffness. The stiffness matrix of this sandwich beam (with the classical six degrees of freedom) has the form (16):

$$\mathbf{K} = \tag{16}$$

$$= \begin{bmatrix} \frac{E_{\mathrm{LN}i}\,A}{b'_{2\mathrm{AEN}}} & 0 & 0 & -\frac{E_{\mathrm{LN}i}\,A}{b'_{2\mathrm{AEN}}} & 0 & 0 \\ 0 & c_{\mathrm{M}}\,b'_{2\mathrm{EIM}} & c_{\mathrm{M}}\,b'_{3\mathrm{EIM}} & 0 & -c_{\mathrm{M}}\,b'_{2\mathrm{EIM}} & c_{\mathrm{M}}\,b_{2\mathrm{EIM}} \\ 0 & c_{\mathrm{M}}\,b'_{3\mathrm{EIM}} & c_{\mathrm{M}}\,(L\,b'_{3\mathrm{EIM}} - b_{3\mathrm{EIM}}) & 0 & -c_{\mathrm{M}}\,b'_{3\mathrm{EIM}} & c_{\mathrm{M}}\,b_{3\mathrm{EIM}} \\ -\frac{E_{\mathrm{LN}i}\,A}{b'_{2\mathrm{AEN}}} & 0 & 0 & \frac{E_{\mathrm{LN}i}\,A}{b'_{2\mathrm{AEN}}} & 0 & 0 \\ 0 & -c_{\mathrm{M}}\,b'_{2\mathrm{EIM}} & -c_{\mathrm{M}}\,b'_{3\mathrm{EIM}} & 0 & c_{\mathrm{M}}\,b'_{2\mathrm{EIM}} & -c_{\mathrm{M}}\,b_{2\mathrm{EIM}} \\ 0 & c_{\mathrm{M}}\,b_{2\mathrm{EIM}} & c_{\mathrm{M}}\,b_{3\mathrm{EIM}} & 0 & -c_{\mathrm{M}}\,b_{2\mathrm{EIM}} & c_{\mathrm{M}}\,(L\,b_{2\mathrm{EIM}} - b_{3\mathrm{EIM}}) \end{bmatrix}$$

where $c_{\mathrm{M}} = E_{\mathrm{LM}i}\,I/(b_{2\mathrm{EIM}}\,b'_{3\mathrm{EIM}} - b_{3\mathrm{EIM}}\,b'_{2\mathrm{EIM}})$ is the bending stiffness parameter. I is a quadratic area moment of inertia of the whole cross-sectional area A. The transfer constants $b'_{2\mathrm{AEN}}$ and $b'_{2\mathrm{EIM}}$, $b'_{3\mathrm{EIM}}$, $b_{2\mathrm{EIM}}$, $b_{3\mathrm{EIM}}$ (these constants can be calculated using the algorithm in [10, 11]) depend on the cross-sectional characteristics and the effective longitudinal elasticity modulus variation for stretching (marked with the index N) and flexural bending (marked with the index M), respectively.

The strains due to longitudinal loading are constant over the cross-section high but non-linear along the beam length axis. The axial stresses are constant over each layer cross-section, but there is a jump in the stresses at the face/core interfaces. If we define the second derivative of the transfer function for stretching $b_{2\mathrm{AEN}}$ as

$$b''_{2\mathrm{AEN}}(x) = \frac{1}{\eta_{\mathrm{AEN}}(x)}\ , \tag{17}$$

than its first derivative is

$$b'_{2\mathrm{AEN}}(x) = \int_0^x b''_{2\mathrm{AEN}}(x)\,\mathrm{d}x\ . \tag{18}$$

The transfer constant for stretching is then

$$b'_{2\mathrm{AEN}} = b'_{2\mathrm{AEN}}(L) = \int_0^L b''_{2\mathrm{AEN}}(x)\,\mathrm{d}x \ . \tag{19}$$

If the polynomial $\eta_{\mathrm{AEN}}(x) = 1$, which means $E^{\mathrm{N}}_{\mathrm{L}}(x) = E_{\mathrm{LN}i} = \text{const.}$, then $b'_{2\mathrm{AEN}}(x) = x$ and $b'_{2\mathrm{AEN}} = L$.

The axial displacement at the point x could be expressed using the new shape functions for a beam with varying stiffness [12, 13]:

$$u(x) = \left(1 - \frac{b'_{2\mathrm{AEN}}(x)}{b'_{2\mathrm{AEN}}}\right) u_i + \frac{b'_{2\mathrm{AEN}}(x)}{b'_{2\mathrm{AEN}}}\, u_j \ . \tag{20}$$

From (19) we get the expression for the axial strains (due to in-plane loading):

$$\varepsilon^{\mathrm{N}}(x) = \frac{\mathrm{d}u(x)}{\mathrm{d}x} = \frac{u_j - u_i}{\eta_{\mathrm{AEN}}(x)\, b'_{2\mathrm{AEN}}} \ . \tag{21}$$

The longitudinal variation of stretching stresses in the layers will be non-linear along the beam length axis

$$\begin{aligned} \sigma^{\mathrm{N}}_1(x) &= \varepsilon^{\mathrm{N}}(x)\, E_1(x) = \sigma^{\mathrm{N}}_3(x) \ , \\ \sigma^{\mathrm{N}}_2(x) &= \varepsilon^{\mathrm{N}}(x)\, E_2(x) \ . \end{aligned} \tag{22}$$

The bending strains vary linearly with y over the whole cross-section and non-linearly along the beam length axis. The advanced flexural sandwich beam rigidity, according the laminate theory [6], is

$$D(x) = b\left(\frac{E^{\mathrm{f}}(x)\,(h^{\mathrm{f}})^3}{6} + \frac{E^{\mathrm{f}}(x)\,h^{\mathrm{f}}\,(h^{\mathrm{c}} + h^{\mathrm{f}})^2}{2} + \frac{E^{\mathrm{c}}(x)\,(h^{\mathrm{c}})^3}{12}\right) \tag{23}$$

and the bending strains are:

$$\varepsilon^{\mathrm{M}}(x, y) = \frac{M(x)}{D(x)}\, y \ , \tag{24}$$

where $M(x)$ is the bending moment at point x.

The bending stresses vary transversal linearly (with the y position) within each layer, but there is a jump in the stresses at the face/core interfaces:

$$\begin{aligned} \sigma^{\mathrm{M}}_1(x, y) &= M(x)\,\frac{E_1(x)}{D(x)}\, y = \sigma^{\mathrm{M}}_3(x, y) \ , \\ \sigma^{\mathrm{M}}_2(x, y) &= M(x)\,\frac{E_2(x)}{D(x)}\, y \ . \end{aligned} \tag{25}$$

The longitudinal variation of the layers bending stress will be non-linear as usual.

The shear stresses for the core and the faces, according to the laminate theory [6], can be calculated using the following expressions ($Q(x)$ is the shear force at point x):

$$\begin{aligned} \tau^{\mathrm{c}}(x, y) &= \frac{Q(x)}{D(x)}\left(\frac{E^{\mathrm{f}}(x)\,h^{\mathrm{f}}\,d}{2} + \frac{E^{\mathrm{c}}(x)}{2}\left(\frac{(h^{\mathrm{c}})^2}{4} - y^2\right)\right) \ , \\ \tau^{\mathrm{f}}(x, y) &= \frac{Q(x)}{D(x)}\,\frac{E^{\mathrm{f}}(x)}{2}\left(\frac{(h^{\mathrm{c}})^2}{4} + h^{\mathrm{c}}\,h^{\mathrm{f}} + (h^{\mathrm{f}})^2 - y^2\right) \ . \end{aligned} \tag{26}$$

The maximum shear stress appears at the neutral axis and it is described by the function:

$$\tau_{\max}(x) = \tau^{\mathrm{c}}(x, y = 0) = \frac{Q(x)}{D(x)} \left(\frac{E^{\mathrm{f}}(x)\, h^{\mathrm{f}}\, d}{2} + \frac{E^{\mathrm{c}}(x)(h^{\mathrm{c}})^2}{8} \right) . \tag{27}$$

The shear stress in the core/face interface is described by the function:

$$\tau^{\mathrm{c}}_{\min}(x, y = h^{\mathrm{c}}/2) = \tau^{\mathrm{f}}_{\max}(x, y = h^{\mathrm{c}}/2) = \frac{Q(x)}{D(x)} \frac{E^{\mathrm{f}}(x)\, h^{\mathrm{f}}\, d}{2} . \tag{28}$$

There is no jump in the shear stresses at the interfaces, and the shear stresses are zero at the outer fibres of the faces.

Example 4:

The following academic parameters have been chosen for the sandwich beam (Figure 12):

- the cross-section is square ($b \times h = 0.01 \times 0.01\,\mathrm{m}$), its area is $A = 0.0001\,\mathrm{m}^2$, $I = 8.3334 \times 10^{-8}\,\mathrm{m}^4$ is the quadratic area moment of inertia, the length of the beam is $L = 1\,\mathrm{m}$;
- the cross-section area of layers is: $A_1 = A_2 = A_3 = A/3 = 3.3334 \times 10^{-5}\,\mathrm{m}^2$
- the effective longitudinal elasticity modulus of layers is:

$$E_1(x) = E_3(x) = E^{\mathrm{f}}(x) = 1 \times 10^{10}\,(1 + x)\,[\mathrm{Pa}],$$
$$E_2(x) = E^{\mathrm{c}}(x) = 2 \times 10^{10}\,(1 + 2\,x)\,[\mathrm{Pa}].$$

The whole beam was modelled with only one of our sandwich beam element. Two load cases have been considered.

Load case 1

In the first load case the longitudinal displacement $u_j = 0.001\,\mathrm{m}$ was prescribed at the free end of the cantilever sandwich beam. Distribution of the longitudinal stress has been searched in the beam layers.

In our case, the effective longitudinal elasticity modulus for stretching (14) of the sandwich beam, $E^{\mathrm{N}}_{\mathrm{L}}(x) = 1.3334 \times 10^{10}\,(1 + 1.5\,x)\,[\mathrm{Pa}]$, changes linearly, where $E_{\mathrm{LN}i} = 1.3334 \times 10^{10}\,\mathrm{Pa}$ and $E_{\mathrm{LN}j} = 3.3334 \times 10^{10}\,\mathrm{Pa}$.

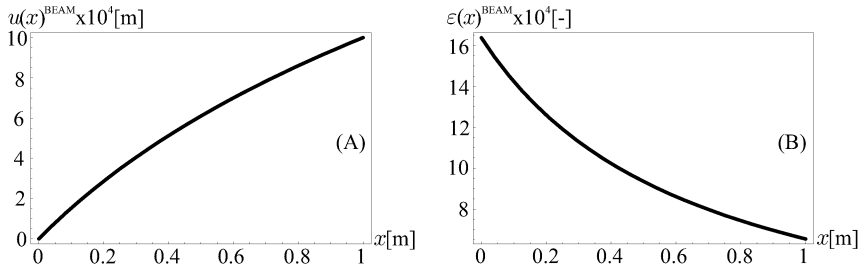

Fig.13: Displacements (A) and strains distribution (B) along the beam length

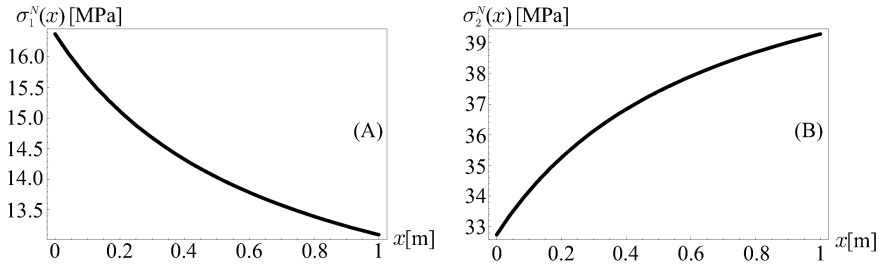

Fig.14: Longitudinal stress distribution in layers 1 and 3 (A), and layer 2 (B)

Figure 13 shows the non-linear displacement and the strain distribution along the beam length. Figure 14 shows the non-linear distribution of the normal stresses in the layers. The middle layer is loaded the most and the maximal stress is placed at its free end (3.9289×10^7 Pa); the layers 1 and 3 have the same stress distribution and the maximal stress is placed at their clamped ends (1.6370×10^7 Pa). The equilibrium equation is satisfied at each position of x; the average normal stress is equal to 2.1827×10^7 Pa and it is constant over the sandwich beam length. This average stress has a virtual meaning only. Normal stresses in the layers have a crucial meaning for the beam strength assessment.

To compare the above-described results, the 4800 of SOLID45 finite elements have been used for solution of this problem (see Figure 15). Figure 16 shows the axial displacements and the axial strains difference distribution obtained using this fine mesh.

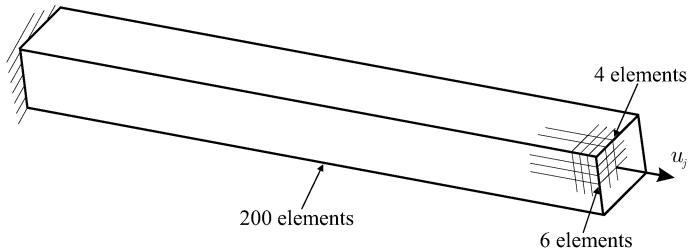

Fig.15: SOLID45 – FE model of the sandwich beam

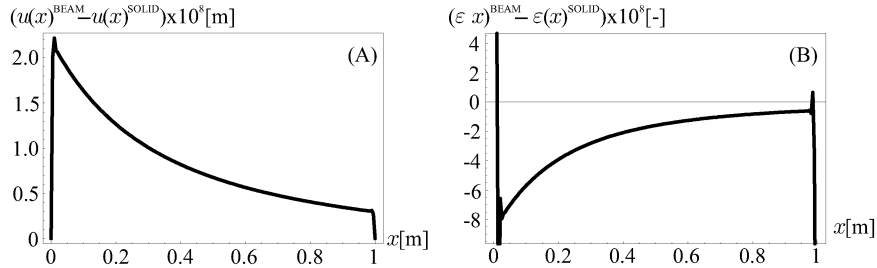

Fig.16: Difference of the axial displacements (A) and strains (B) between results achieved using BEAM and SOLID elements

How it can be seen from these figures, that the analysis results using this SOLID45 finite element mesh were in a very good agreement with only one our new beam element results.

Load case 2

In the second load case the transversal unit force ($F = 1\,\mathrm{N}$) has been applied at the free end of cantilever sandwich beam (Figure 12). A linear – elastic analysis has been done. The deflection curve and distribution of normal stresses along the beam layers and over the beam depth have been examined.

In this case, the effective longitudinal elasticity modulus for bending (15) of the sandwich beam changes linearly and has this form:

$$E_{\mathrm{L}}^{\mathrm{M}}(x) = 1.037037{\times}10^{10}\,(1 + 1.071428571\,x)\ [\mathrm{Pa}]\ ,$$

where $E_{\mathrm{LM}i} = 1.037037{\times}10^{10}\,\mathrm{Pa}$ and $E_{\mathrm{LM}j} = 2.148148{\times}10^{10}\,\mathrm{Pa}$ (see Figure 17). Using this elasticity modulus, the deflection and rotation at the free beam end is $v_j = -0.031188\,\mathrm{m}$ and $\varphi_j = -0.044056\,\mathrm{rad}$ respectively. As it can be shown, the reactions at node i satisfy the equilibrium equations exactly.

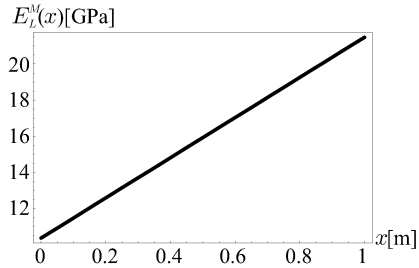

Fig.17: Effective longitudinal elasticity modulus for bending of a sandwich beam

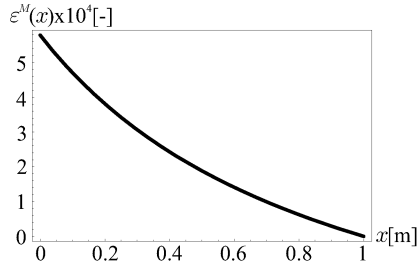

Fig.18: Bending strain distribution at the top of layer 3

The bending strain (24) has been obtained as the following function at the top of the layer 3:

$$\varepsilon^{\mathrm{M}}(x) = \frac{0.005\,(1-x)}{8.6419 + 9.2592\,x}\ .$$

This function is depicted in Figure 18. Its value at note i is 0.0005785. Longitudinal distribution of the bending normal stress (25) is shown in the Figure 19. Figure 19A shows the bending normal stress at the top of the layer 3 and Figure 19B shows the bending normal stress at the top of the layer 2 and bottom of the layer 3. The same problem has been solved using the SOLID45 finite elements (see Figure 15). By this very fine mesh the ANSYS solution converged to our sandwich beam element solution. For example, the deflection at

the free beam end coincided with our value; the maximal normal stress at the top of the layer 1 and 3 (at the clamped beam end) has the value of 5.7689 MPa. The shear stress has been calculated using the expressions (26)–(28). In Figure 20 distribution of the maximal core shear stresses (27) (shear stress at the middle of the layer 2) and the shear stresses at the face/core interfaces (shear stress at the top of the layer 2 and shear stress at the bottom of the layer 3) are shown along the beam length.

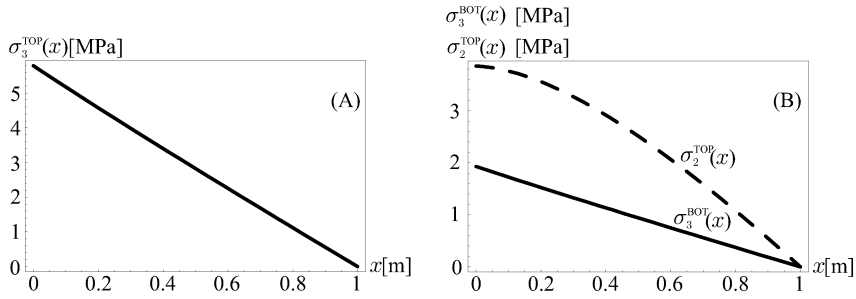

Fig.19: Longitudinal distributions of the bending normal stress

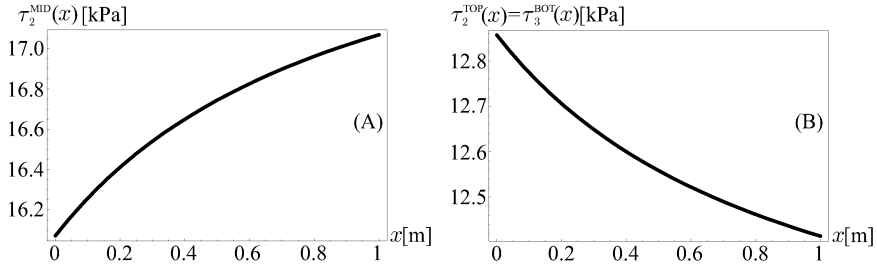

Fig.20: Longitudinal distribution of the maximal core shear stress and the shear stress at the face/core interfaces

Maximal core shear stress in the both ends are: $\tau^{\mathrm{c}}(x=0, y=0) = 16071.4\,\mathrm{Pa}$; $\tau^{\mathrm{c}}(x=L, y=0) = 17068.9\,\mathrm{Pa}$ and the values of stress at the face/core interfaces at the same nodal points are: $\tau^{\mathrm{c}}_{\min}(x=0) = \tau^{\mathrm{f}}_{\max}(x=0) = 12857.1\,\mathrm{Pa}$; $\tau^{\mathrm{c}}_{\min}(x=L) = \tau^{\mathrm{f}}_{\max}(x=L) = 12413.7\,\mathrm{Pa}$.

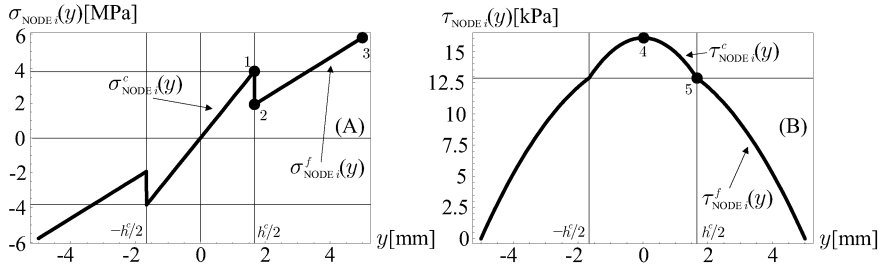

Fig.21: Transversal distribution of the normal and shear stress across the beam depth

The transversal distribution of the normal and shear stresses across the beam depth at the node i is shown in Figure 21. As we can see, there is a jump in the normal stresses at

the face/core interfaces (this stress jump can not be reached using the SOLID45 element because of averaging of the nodal stresses), but there is no jump in shear stresses in this location.

The normal stresses at individual points have these values: point 1 (top of the core): 3.8571 MPa, point 2 (bottom of the face): 1.9285 MPa, point 3 (top of the face): 5.7857 MPa and, between these points, there is a linear distribution of the normal stresses in core $\sigma^{\mathrm{c}}_{\mathrm{NODE}i}(y)$ and in faces $\sigma^{\mathrm{f}}_{\mathrm{NODE}i}(y)$ – see Figure 21.

The shear stresses at individual points have these values: point 4 (middle of the core): 16.0714 kPa, and point 5 (top of the core and bottom of the face): 12.8571 kPa. The shear stress distribution in core is described by

$$\tau^{\mathrm{c}}_{\mathrm{NODE}i}(x=0, y \in \langle 0, h^{\mathrm{c}}/2\rangle) = 16071.4285 - 1.1571{\times}10^{9}\, y^2 \text{ [Pa]}$$

and in the faces by

$$\tau^{\mathrm{f}}_{\mathrm{NODE}i}(x=0, y \in \langle h^{\mathrm{c}}/2, h/2\rangle) = 14464.2857 - 5.7857{\times}10^{8}\, y^2 \text{ [Pa]} .$$

4. Conclusions

Mixture rules have been extended to account for polynomial longitudinal and layer-wise symmetric transversal variation of the composite (FGM's) beam elasticity modulus. Longitudinal variations of the volume fractions of constituents and longitudinal variations of the elasticity moduli of constituents were considered in the first part of this contribution. The material properties were considered constant along the beam width and depth. A constant cross-sectional area can have various geometries but it must be symmetric to the bending (x-y) plane. The symmetric transversal layer-wise stiffness variation of the sandwich beam element was considered in the second part of this paper. Longitudinal variations of the stiffnesses of layers were considered as well by this sandwich beam element. Stiffness matrices of the composite (FGM) Bernoulli-Euler beam finite element and three-layer composite (FGM) sandwich beam finite element have been proposed. They contain the longitudinally varying effective elasticity moduli for axial stretching and transversal bending. The effective longitudinal elasticity moduli of the sandwich beam have been accomplished using the laminate theory (including transverse shear) and homogenisation by using the above mentioned extended mixture rules.

Stiffness matrix of the homogenized sandwich beam contains in-plane, bending and shear stiffness of all layers, i.e. for the faces and core. Any restriction has not been assumed either for thickness of the faces nor for weakness of the core. This new sandwich beam element can be used for analysis of the beams according to the assumptions of the linear elastic beam theory. The bars of analysed beam structure have to be meshed with larger number of the proposed finite elements in the case of longitudinal discontinuity of the material properties, cross-sectional area and loads. The numerical examples have been solved using the advanced mixture rules and the new FGM's beam finite elements with varying stiffness. The analysis results have been evaluated, discussed and compared with those obtained using the common beam and solid finite elements. Implementation of the new sandwich beam element in the existing FEM-cods is very easy. Algorithm for calculation of the transfer constants has to be included additionally into the code. This algorithm is described in the references. Our new

composite sandwich beam finite element can be used not only in the case when the extended mixture rules have been used for homogenization of material properties, but also it can be used for all cases, when the variation of homogenized material properties is known and it can be described with the polynomial function. The new composite beam finite elements are very effective and accurate.

Acknowledgement

This paper has been accomplished under the VEGA grant 1/4122/07.

References

[1] Halpin J.C., Kardos J.L.: The Halpin-Tsai equations. A review, Polymer Engineering and Science 1976; 16(5):344-352.
[2] Mori T., Tanaka K.: Average stress in matrix and average elastic energy of materials with misfitting inclusions, Acta Metall 1973; 21:571–574
[3] Love B.M., Batra R.C.: Determination of effective thermomechanical parameters of a mixture of two elastothermoviscoplastic constituents, International Journal of Plasticity 2006;22:1026 –1061
[4] Fish J., Chen W., Tang Y.: Generalized mathematical homogenisation of atomistic media at finite temperatures, International Journal of Multiscale Computational Engineering 2005;3(4):393–413
[5] Liu W.K., Karpov E.G., Park H.S.: Nano Mechanics and Materials : Theory, Multiple Scale Analysis, and Applications, Springer, 2005
[6] Altenbach H., Altenbach J., Kissing W.: Mechanics of Composite Structural Elements, Springer – Verlag, 2004
[7] Chakraborty A., Gopalakrishnan S., Reddy J.N.: A new beam finite element for the analysis of functionally graded materials, International Journal of Mechanical Sciences 2003;45:519–539
[8] ANSYS 10.1: A general purpose FEM program 2006
[9] Murín J., Kutiš V.: 3D-beam element with continuous variation of the cross-sectional area, Computers and Structures 2002;80(3-4):329–338
[10] Kutiš V., Murín J.: Stability of a slender beam-column with locally varying Young's modulus, Structural Engineering and Mechanics, An International Journal 2006; 23(1):15–27
[11] Rubin H., Schneider K.J.: Baustatik, Werner Verlag, 1996
[12] Murín J., Kutiš V.: Geometrically non-linear truss element with varying stiffness, Engineering Mechanics 2006;13(6):435–452
[13] Murín J., Kutiš V., Masný M.: Link element with varying conductance for thermoelectric analysis, International Journal for Computational Methods in Engineering and Mechanics 2006;7(6):411–423

Received in editor's office: December 27, 2007
Approved for publishing: February 29, 2008